

1 **RESEARCH ARTICLE:**

2 **Quantification of reactive oxygen species production by the red fluorescent proteins**
3 **KillerRed, SuperNova and mCherry.**

4

5 **AUTHORS:**

6 John O. Onukwufor ^{a1}, Adam J. Trewin ^{a1}, Timothy M. Baran ^b, Anmol Almast ^a, Thomas H.
7 Foster ^b, and Andrew P. Wojtovich ^{a*}

8

9 **AFFILIATIONS:**

10 ^a University of Rochester Medical Center, Department of Anesthesiology and Perioperative
11 Medicine, Rochester NY, 14642 United States.

12 ^b University of Rochester Medical Center, Department of Imaging Sciences, Rochester 14642,
13 United States.

14

15 ¹ These authors contributed equally

16 * Corresponding author:

17 Andrew P. Wojtovich

18 Telephone: +1 585 275 4613

19 Email: Andrew_wojtovich@urmc.rochester.edu

20

21

22 **ABSTRACT**

23 Fluorescent proteins can generate reactive oxygen species (ROS) upon absorption of photons
24 via type I and II photosensitization mechanisms. The red fluorescent proteins KillerRed and
25 SuperNova are phototoxic proteins engineered to generate ROS and are used in a variety of
26 biological applications. However, their relative quantum yields and rates of ROS production
27 are unclear, which has limited the interpretation of their effects when used in biological
28 systems. We cloned and purified KillerRed, SuperNova, and mCherry - a related red
29 fluorescent protein not typically considered a photosensitizer - and measured the superoxide
30 ($O_2^{\cdot-}$) and singlet oxygen (1O_2) quantum yields with irradiation at 561 nm. The formation of the
31 $O_2^{\cdot-}$ -specific product 2-hydroxyethidium (2-OHE⁺) was quantified via HPLC separation with
32 fluorescence detection. Relative to a reference photosensitizer, Rose Bengal, the $O_2^{\cdot-}$
33 quantum yield ($\Phi_{O_2^{\cdot-}}$) of SuperNova was determined to be 0.00150, KillerRed was 0.00097,
34 and mCherry 0.00120. At an excitation fluence of 916.5 J/cm² and matched absorption at 561
35 nm, SuperNova, KillerRed and mCherry made 3.81, 2.38 and 1.65 $\mu M O_2^{\cdot-}/min$, respectively.
36 Using the probe Singlet Oxygen Sensor Green (SOSG), we ascertained the 1O_2 quantum yield
37 (Φ^1O_2) for SuperNova to be 0.0220, KillerRed 0.0076, and mCherry 0.0057. These
38 photosensitization characteristics of SuperNova, KillerRed and mCherry improve our
39 understanding of fluorescent proteins and are pertinent for refining their use as tools to
40 advance our knowledge of redox biology.

41

42

43

44 **KEYWORDS:** redox, optogenetics, superoxide, singlet oxygen, photosensitizer, quantum
45 yield.

46

47

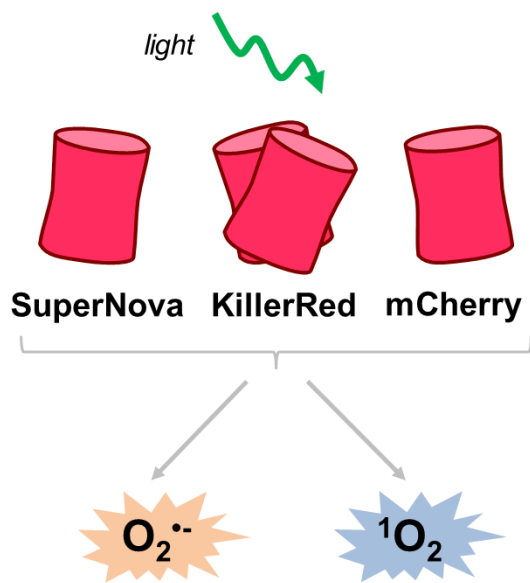
48 **ABBREVIATIONS:**

49	2-OHE ⁺ :	2-hydroxyethidium
50	CALI:	Chromophore assisted light inactivation
51	DHE ⁺ :	Dihydroethidium
52	E ⁺ :	Ethidium
53	O ₂ ^{•-} :	Superoxide
54	¹ O ₂ :	Singlet oxygen
55	Φ:	Quantum yield
56	ΦO ₂ ^{•-} :	Superoxide quantum yield
57	Φ ¹ O ₂ :	Singlet oxygen quantum yield
58	ROS:	Reactive oxygen species
59	SOSG:	Singlet oxygen sensor green
60	SOD:	Superoxide dismutase
61	X:	Xanthine
62	XO	Xanthine oxidase

63

64

65 **GRAPHICAL ABSTRACT**



66

67

68

69 INTRODUCTION

70 Fluorescent proteins generate reactive oxygen species (ROS) upon irradiation by type
71 I or type II photosensitization mechanisms [1-4]. The type I mechanism involves electron
72 transfer reactions that ultimately reduce molecular oxygen to form superoxide ($O_2^{\cdot-}$) [3, 5].
73 Type II photosensitization involves the direct energy transfer from excited triplet state of the
74 photosensitizer to oxygen to generate singlet oxygen (1O_2) [4-7]. Both $O_2^{\cdot-}$ and 1O_2 can be
75 formed by fluorescent proteins [4, 5] but the relative yields or fluxes depend on various factors,
76 including the protein structure surrounding the chromophore, the oxygen concentration,
77 temperature, and pH of the environment [3, 5].

78 A range of phototoxic fluorescent proteins have been developed such as KillerRed,
79 KillerOrange, SuperNova, miniSOG and their derivatives; however their phototoxic properties
80 are not fully characterized [1-3, 8-11]. KillerRed, a dimeric red fluorescent protein, was derived
81 from a random and site-directed mutations of a jellyfish protein, anm2CP [1, 3, 10, 12].
82 KillerRed has a unique structure with a water channel to the chromophore that is responsible
83 for its phototoxicity [1, 3, 10, 12]. The original KillerRed protein is prone to variable levels of
84 dimerization, which can lead to artifacts and mislocalization of fusion proteins within a
85 biological system [8]. These confounding factors can be mitigated by using the pseudo-
86 monomeric version tandem KillerRed (tdKillerRed), which consists of two repeats of the
87 KillerRed coding sequence, meaning that all copies are expressed as a dimer. SuperNova
88 was derived from KillerRed and retains similar phototoxic properties but exists as a monomer,
89 thereby limiting potential mislocalization events [8]. Both KillerRed and SuperNova are used
90 in a variety of applications ranging from localized ROS production to cell ablation, however
91 the quantities or the species of ROS responsible for the effect are often unclear. KillerRed has
92 been used for chromophore- assisted light inactivation (CALI) in cells and organelles [1, 13-
93 16]. These phototoxic effects have been shown to be sensitive to superoxide dismutase
94 (SOD), catalase, and sodium azide [1, 8], suggesting that KillerRed possesses the capacity to
95 generate both $O_2^{\cdot-}$ (and subsequently hydrogen peroxide) and 1O_2 oxidants [1, 2, 8]. Likewise,

96 SuperNova has been shown to oxidize DHE and ADPA probes, implying that it too generates
97 both $O_2^{\cdot-}$ and 1O_2 oxidants [8, 17].

98 Although the phototoxic effects of these fluorescent proteins to cellular functioning
99 have been widely demonstrated, their precise ROS quantum yields, i.e. the ratio of ROS
100 molecules generated per photon absorbed by the fluorophore, and intrinsic rates of ROS
101 production have not previously been reported. Therefore, the aim of this study was to
102 determine the quantum yields and rates of ROS production by phototoxic fluorescent proteins.
103 Using Rose Bengal, a well-characterized chemical photosensitizer molecule with a defined
104 $O_2^{\cdot-}$ quantum yield ($\Phi_{O_2^{\cdot-}}$) of 0.2 and 1O_2 quantum yield (Φ^1O_2) of 0.75 as a standard [18], we
105 determined the relative $O_2^{\cdot-}$ and 1O_2 quantum yields of KillerRed and SuperNova. As a
106 negative control for photosensitization we used mCherry, a red fluorescent protein commonly
107 used as an 'inert' fluorophore in many cellular imaging applications [3, 8]. Overall, we report
108 the $O_2^{\cdot-}$ and 1O_2 quantum yield of the fluorescent proteins tdKillerRed and SuperNova, as well
109 as mCherry.

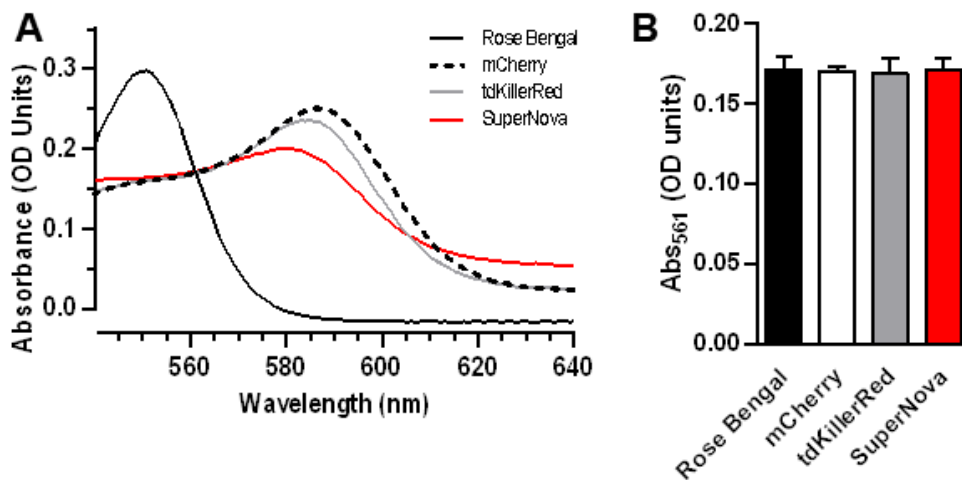
110

111 **MATERIALS AND METHODS**

112 **Protein cloning and purification**

113 SuperNova, tdKillerRed, and mCherry were transformed and grown in a culture as
114 previously described [8, 17]. SuperNova/pRSETB was a gift from Dr. Takeharu Nagai
115 (Addgene plasmid # 53234) [8]. mCherry (pmCherry-C1) and tdKillerRed (#FP963, Evrogen)
116 were amplified and ligated into pRSETB using BamHI and EcoRI. Plasmids were then
117 transfected into JM109 (DE3) XJ autolysis cells, and protein expression was induced with
118 isopropyl β -D-1-thiogalactopyranoside (IPTG). Cultures were centrifuged at 3200 g for 10 min,
119 washed with PBS and flash frozen. Cell lysate was run through nickel beads, then protein was
120 eluted with 100 μ M imidazole in the presence of protease inhibitors (Roche) and desalted
121 using a PD-10 column. Protein concentration was determined by Lowry assay, and

122 absorbance scans were performed on a spectrophotometer (Shimadzu) to identify a region of
123 spectral overlap in absorbance maxima between the proteins and Rose Bengal dye (# 330000,
124 Sigma). The most robust overlap occurred between 550-580 nm (Fig. 1). Based on this, a 561
125 nm laser was chosen for subsequent experimentation. Proteins and Rose Bengal were diluted
126 to achieve equal molar absorptivity at 561 nm using the Beer-Lambert equation ($A=\epsilon*b*c$).
127



128
129 Fig. 1. **Equal photosensitizer absorbance at 561 nm.** (a) Absorbance spectrum of photosensitizers. (b)
130 Absorbance at 561 nm after adjustment of concentration of Rose Bengal dye (0.0026 mg/mL), mCherry (0.22
131 mg/mL), tdKillerRed (0.25 mg/mL), and SuperNova (0.76 mg/mL). Values are mean \pm SD for n = 3 independent
132 experiments; p > 0.05 by one-way ANOVA.

133

134 Irradiation parameters

135 Irradiation of fluorescent proteins and the photosensitizing dye, Rose Bengal, were
136 performed using a 561 nm class IIIb 50 mW diode laser (#1230935, Coherent® OBIS™,
137 Edmund Optics, NJ, USA). The 0.7 mm diameter beam was focused through a 20x, 0.4 NA
138 microscope objective lens (Swift) into a 200 μ m core diameter, 0.22 NA SMA-terminated fiber
139 optic cable (Part # M25L05, ThorLabs, Inc., Newton, NJ) for delivery to the sample. The fiber
140 and objective lens were positioned using a Multimode Fiber Coupler Assembly (Part # F-91-

141 C1-T, Newport Corporation, Irvine, CA). Fiber output was collimated with an aspheric lens
142 (Part # A397TM-B, Thorlabs) to create a 2.5 mm-diameter collimated beam to irradiate each
143 200 μ L sample volume contained within a 1.5 mL, 1 cm polystyrene cuvette (#97000-586,
144 VWR). The irradiance was measured as 25 mW at the front surface of the sample cuvette
145 using thermopile detector (818P-010-12, Newport Corporation, Irvine, CA) for all irradiation.
146 Fluence/light dose (J/cm^2) was modulated by adjusting irradiation time while maintaining a
147 consistent fluence rate (mW/cm^2).

148

149 **Determination of photobleaching rates**

150 Photobleaching rates of photosensitizers (Rose Bengal, 0.0026 mg/ml; mCherry, 0.22
151 mg/ml; KillerRed, 0.25 mg/ml; SuperNova, 0.76 mg/ml) and the probe DHE alone and in
152 combinations were determined in buffer (D-MRB; 220 mM Manitol, 70 mM Sucrose, 5 mM
153 MOPS, 2 mM EGTA, 0.4% FFBSA, 0.1 mM DTPA, pH 7.3) at 20 °C. The fluorescence signal
154 (Ex 525 nm; Em 550 nm) was acquired using a fluorescence spectrophotometer (Cary Eclipse,
155 Agilent Technologies) during a cumulative time exposure (0-30 min) at 561 nm irradiation for
156 determination of the reduction in fluorescence. To determine the bleaching rates with SOSG,
157 DHE was replaced with SOSG in the buffer, and the change in absorbance was measured
158 between 400 – 800 nm using a spectrophotometer.

159

160 **Xanthine oxidase superoxide production**

161 Xanthine oxidase (XO) production of $\text{O}_2^{\cdot-}$ was determined as the rate of SOD-sensitive
162 cytochrome *c* reduction, as previously described [7, 19]. Briefly, XO (0.25, 0.50, 1.0 and 4.0
163 mU/mL) was added to a 1 cm cuvette containing cytochrome *c* (40 μ M) in PBS containing
164 DTPA (D-PBS: 7.78 mM Na_2HPO_4 , 2.20 mM KH_2PO_4 , 0.1 mM DTPA, pH 7.3). All reactions
165 were carried out at ambient O_2 and where indicated catalase (4200 U/mL) or SOD (800 U/mL)
166 was present. Baseline was collected for 2 min before 1 mM of xanthine (X) was added to

167 initiate the reaction. Cytochrome c reduction was monitored at 550 nm for 10 min, and the rate
168 was calculated using an extinction coefficient of $18.7 \text{ mM}^{-1} \text{ cm}^{-1}$ [20].

169

170 **Superoxide quantification**

171 The oxidation of dihydroethidium (DHE) yields the $\text{O}_2^{\cdot-}$ specific fluorescence product 2-
172 hydroxyethidium (2-OHE⁺) along with non-specific fluorescent products including ethidium
173 (E⁺), which were separated using HPLC as previously described [7, 17, 21, 22]. Briefly, XO (4
174 mU/mL) and X (1 mM) were incubated in D-PBS at 20 °C for the indicated time (0 – 60 min).
175 Rose Bengal (0.0026 mg/mL), mCherry (0.22 mg/ml), tdKillerRed (0.25 mg/ml), or SuperNova
176 (0.76 mg/ml) were irradiated at 561 nm for the indicated time (0 – 30 min) in D-MRB in the
177 presence of DHE (100 μM). For experiments containing photosensitizers, the absorbance was
178 measured (400-800 nm) both pre- and post-irradiation at 561 nm. To these samples, an equal
179 volume of 200 mM $\text{HClO}_4/\text{MeOH}$ was added, centrifuged at $17,000 \times g$, and the supernatant
180 transferred to an equal volume 1 M K^+PO_4^- at pH 2.6.

181 Samples were separated using a Polar-RP column (Phenomenex, 150 x 2 mm; 4 μm) on a
182 Shimadzu HPLC with fluorescence detection (RF-20A). The flow rate was constant (0.1
183 mL/min) using a gradient of two mobile phases (A: 10% ACN, 0.1 %TFA; B: 60% ACN, 0.1
184 %TFA). The gradient was the following: 0 min, 40% B; 5 min, 40% B; 25 min, 100% B; 30 min,
185 100% B; 35 min, 40% B; 40min, 40% B. Standard curves were generated against known
186 concentrations of E⁺ and 2-OHE⁺, and peaks were quantified using Lab Solutions (Shimadzu)
187 [7, 17].

188

189 **Singlet oxygen quantification**

190 The $^1\text{O}_2$ production of photosensitizers (Rose Bengal, 0.0026 mg/mL; mCherry, 0.22
191 mg/ml; KillerRed, 0.25 mg/ml; SuperNova, 0.76 mg/ml) was measured using SOSG (1 μM ,

192 #S36002, Invitrogen) in D-MRB at 20°C [7]. The SOSG signal (Ex 525 nm; Em 550 nm) was
193 acquired using a Cary Eclipse fluorescence spectrophotometer (Agilent Technologies) pre-
194 and post- 561 nm irradiation for determination of the change in SOSG fluorescence intensity
195 [7].

196

197 **Calculations and statistical analysis**

198 Fluorescent protein O₂⁻ and ¹O₂ quantum yields were determined after correcting for
199 the bleaching rates of the photosensitizers, as we have previously demonstrated the
200 importance of photobleaching in explaining time-dependent ROS production by
201 photosensitizers [23]. Measurements of fluorescence/absorbance vs. illumination duration
202 were first normalized to the value prior to illumination, and then fit with an equation of the form
203 $B(t) = ae^{-bt}$, where a and b are fit coefficients and t is the illumination duration in seconds.

204 The total number of absorbed photons for a sample can then be expressed as $A =$
205 $A_0 \int_0^{t_d} B(t)dt$, where A_0 is the absorption prior to illumination, t_d is the illumination duration,
206 and $B(t)$ is the bleaching curve described above. Relative to a reference quantum yield (Φ_R),

207 the quantum yield of a sample (Φ_S) can be determined by $\Phi_S = \frac{out_S/A_S}{out_R/A_R} \cdot \Phi_R$, where out is the

208 output of interest and A is the total number of absorbed photons, as described above.

209 Incorporating correction for bleaching of the sample and reference, with knowledge that pre-
210 illumination (A_0) is equal for all samples, the quantum yield can be expressed as:

$$211 \quad \Phi_S = \frac{out_S}{out_R} \cdot \frac{\int_0^{t_R} B_R(t)dt}{\int_0^{t_S} B_S(t)dt} \cdot \Phi_R,$$

212 where out_S and out_R are measured outputs for illumination durations of t_S and t_R for the sample
213 and reference, respectively, and B_S and B_R are the corresponding bleaching curves. All fitting
214 and calculation was performed in MATLAB (The MathWorks, Inc., Natick, MA).

215

216 $O_2^{\cdot -}$ production rates of the fluorescent proteins were calculated based upon the
217 standard curve generated using X/XO. Since the apparent number of $O_2^{\cdot -}$ molecules required
218 to generate one 2-OHE⁺ molecule is dependent on the rate of $O_2^{\cdot -}$, photosensitizer $O_2^{\cdot -}$
219 production was matched with 4 mU/mL XO superoxide generation. Under these conditions
220 X/XO produced 2.24 μ M $O_2^{\cdot -}$ /min. X/XO was incubated (0-60 min) of DHE and 2-OHE⁺ was
221 measured and plotted against the expected cumulative $O_2^{\cdot -}$ concentration generated during
222 that time, as previously described [7]. At these lower rates the ratio of $O_2^{\cdot -}$ to 2-OHE⁺ was
223 linear ($y = 55.62(x) + 326.2$; $R^2 = 0.98$).

224 Statistical analysis: Data were first tested for normality of variance, and were then
225 analyzed by one- or two-way ANOVA with Tukey's post hoc using GraphPad Prism (v7).

226

227 RESULTS

228 *Purification and characterization of fluorescent proteins.*

229 Fluorescent proteins subjected to SDS-PAGE migrated at their expected molecular
230 weight (Supplemental Fig. 1). In order to measure protein photosensitization characteristics
231 relative to a reference dye (Rose Bengal), we first sought to determine i) a wavelength that
232 was near the absorption maxima for each chromophore, ii) a concentration of each
233 chromophore in solution that would allow all of the photosensitizers absorb an equal number
234 of photons and iii) is not confounded by absorption of photons by other reagents used for
235 detection of ROS. We determined from absorbance spectra that excitation at 561 nm met each
236 of these criteria (Fig. 1A), and photosensitizer concentrations were then optically matched for
237 equal absorbance at 561 nm (Fig. 1B).

238

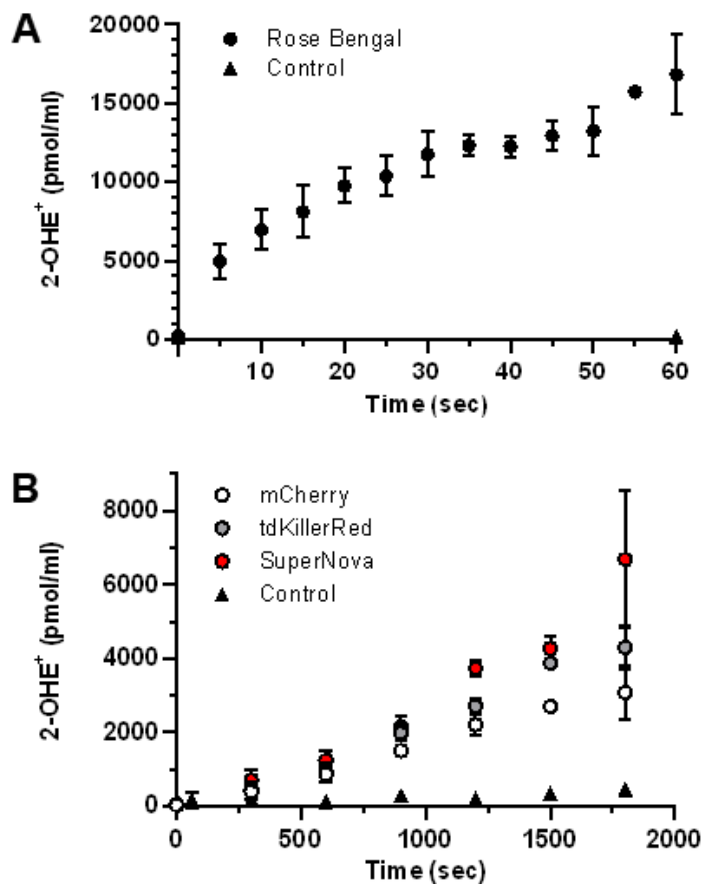
239

240

241

242 ***Superoxide quantum yield and superoxide generation rate of fluorescent proteins***

243 We measured light-dependent photosensitizer $O_2^{\cdot-}$ generation using HPLC to quantify
244 2-OHE⁺, a $O_2^{\cdot-}$ specific reaction product of DHE [7, 24-26]. Since the known yield of Rose
245 Bengal served as our reference, we confirmed that Rose Bengal produced 2-OHE⁺ in a light
246 dose-dependent manner (Fig. 2A). Similarly, the fluorescent proteins tdKillerRed, SuperNova
247 and mCherry also produced 2-OHE⁺ in a light dose-dependent manner (Fig. 2B), yet the
248 magnitude of 2-OHE⁺ for the protein photosensitizers was considerably lower than that of
249 Rose Bengal. For example, after 60 seconds of illumination Rose Bengal generated ~17,000
250 pmol/mL 2-OHE⁺, while after 300 seconds the fluorescent proteins produced ~500 pmol/mL
251 (Fig. 2B).



252

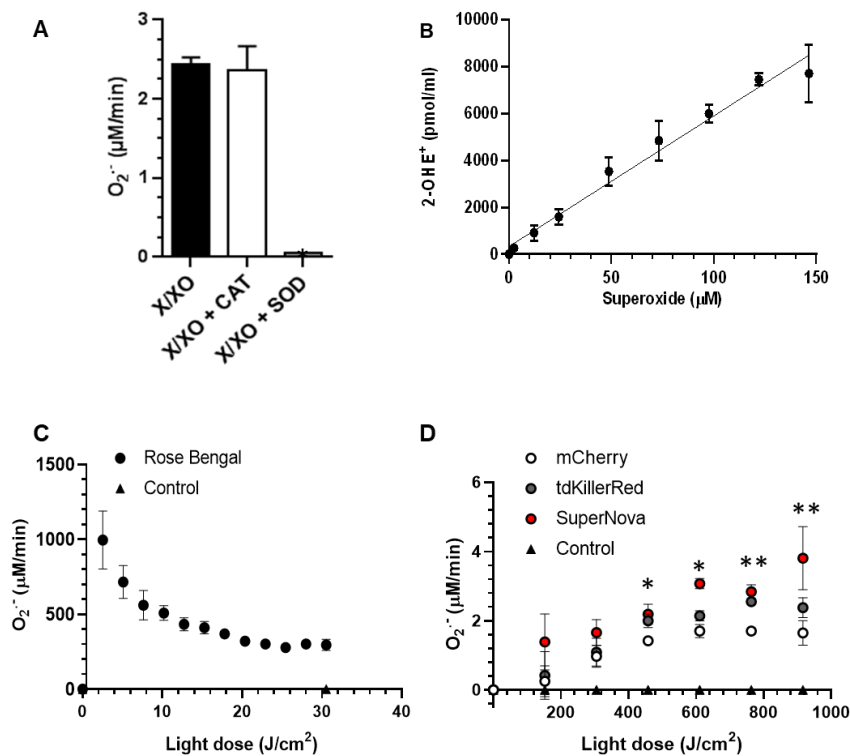
253 Fig. 2. **Light-dependent superoxide generation by photosensitizers.** (a) Rose Bengal, (b) tdKillerRed,
254 Supernova, mCherry and control (no photosensitizer) were irradiated with equal molar absorptivity at 561 nm in
255 the presence of DHE (100 μ M) for quantification of 2-OHE⁺. Values are mean \pm SD for n = 3 independent
256 experiments.

257

258 Next, we sought to determine the O₂⁻ quantum yield of tdKillerRed, SuperNova and
259 mCherry relative to Rose Bengal, with a known $\Phi_{O_2^-}$ of 0.2 [18]. The determination of quantum
260 yields relies on the equal absorbance of photons, yet photobleaching results in a decrease in
261 photon absorbance over time that occurs at different rates between photosensitizers. We
262 therefore measured the rate of photosensitizer bleaching by assessing the change in
263 fluorescence in response to a cumulative light-dose. We then corrected for the bleaching rates
264 of the individual fluorophores and the probe, DHE, (Supplemental Fig. S2) in order to calculate
265 the $\Phi_{O_2^-}$ relative to Rose Bengal. We thus determined that SuperNova had a $\Phi_{O_2^-}$ of 0.0015,
266 and tdKillerRed's $\Phi_{O_2^-}$ was 0.00097; mCherry had a comparable $\Phi_{O_2^-}$ (Table 1).

267 We next sought to calculate the O₂⁻ production rate of fluorophores. However, the
268 apparent ratio of O₂⁻ molecules necessary to form one molecule of 2-OHE⁺ is highly
269 dependent of the rate of O₂⁻ generation, possibly due to competition with spontaneous
270 dismutation [7, 26]. Therefore, we generated a standard curve using a concentration of
271 xanthine oxidase that produces O₂⁻ at a similar rate to that of the photosensitizers. Based on
272 the results of the dose response (Supplementary Fig. S3), we selected 4 mU/mL of xanthine
273 oxidase (Fig. 3A) to match the 2-OHE⁺ production rates from our photosensitizers at this
274 concentration and light dose. We determined that 4 mU/mL of xanthine oxidase produces 2.44
275 μ M/min of O₂⁻, which was SOD-sensitive and catalase-insensitive (Fig. 3A). We incubated the
276 same amount of xanthine oxidase in the presence of DHE and measured the formation 2-
277 OHE⁺ over time and expressed it as a function of expected cumulative O₂⁻ production. Our
278 results show a linear increase of 2-OHE⁺ with increasing amounts of O₂⁻ across the tested
279 range ($R^2 = 0.98$; Fig. 3B). Given that the photosensitizers absorbed an equal amount of light

280 and hence have the same ability to make ROS (Fig. 1), we then used this equation to derive
 281 the rate of $O_2^{\cdot-}$ production by photosensitizers per unit light dose (Fig. 3C & D) from the data
 282 in Fig. 2. Rose Bengal had the highest rates of $O_2^{\cdot-}$ production across light doses ($\sim 300 \mu M$
 283 $O_2^{\cdot-}$ /min at $30.55 J/cm^2$) with mCherry producing the least amount $O_2^{\cdot-}$ per light dose (~ 1.65
 284 $\mu M O_2^{\cdot-}$ /min at $916.5 J/cm^2$) (Fig. 3C & D). The rate of $O_2^{\cdot-}$ production by Rose Bengal
 285 decreased with increasing light dose, which is consistent with the bleaching rate of Rose
 286 Bengal (Supplemental Fig. 2). The progressive loss of absorption resulted in a fluence-
 287 dependent decrease in the $O_2^{\cdot-}$ production rate. At the light doses tested, each of the
 288 fluorescent proteins showed an increasing $O_2^{\cdot-}$ production rate that reached a plateau around
 289 $600 J/cm^2$ (Fig. 3D). The gradual increase in the measured $O_2^{\cdot-}$ production rate could be due
 290 to saturation of local reaction sites, such as amino acids, that can quench ROS, or a
 291 conformational change in the protein resulting in a maximal observed production rate, as has
 292 been reported for other fluorescent proteins [27]. As the fluorescent proteins bleach at a slower
 293 rate compared to Rose Bengal (Supplemental Fig. 2), we did not observe the same decrease
 294 in $O_2^{\cdot-}$ production rate that was observed for Rose Bengal.



295

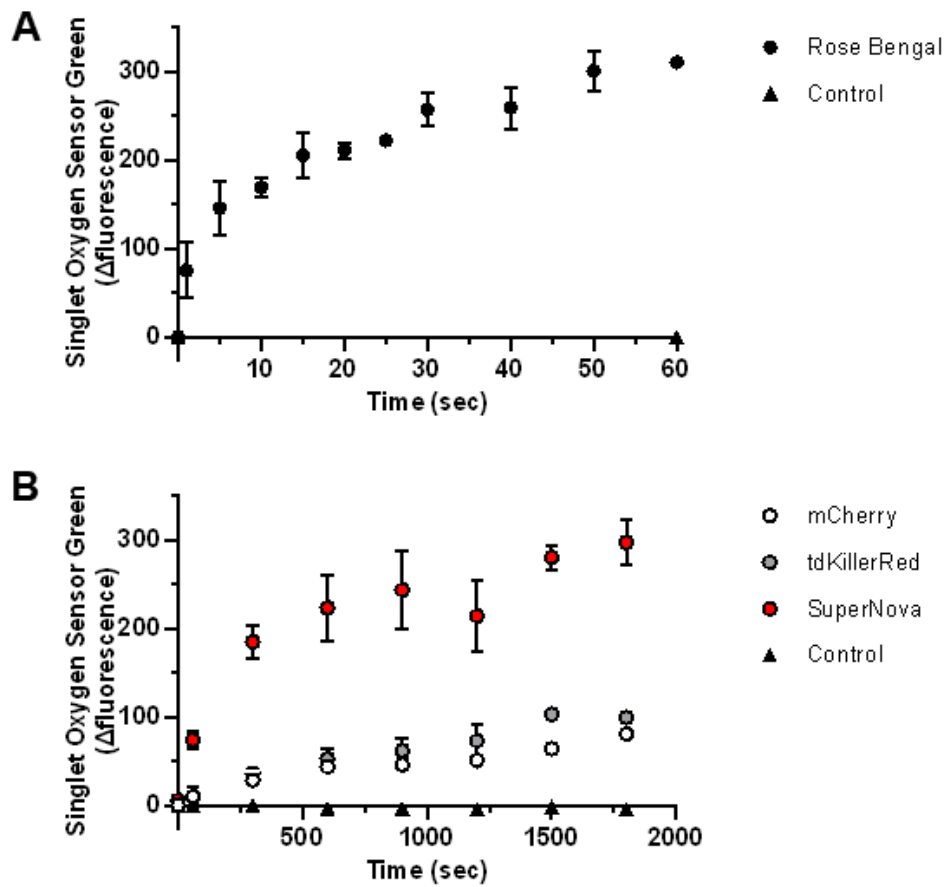
296 Fig. 3. **Determination of superoxide production per light dose.** (a) xanthine/xanthine oxidase (X/XO) $O_2^{\cdot-}$
297 production was assessed using cytochrome c reduction assay. Xanthine oxidase (XO, 4 mU/mL) and xanthine (X,
298 1 mM) were incubated with catalase (CAT) superoxide dismutase (SOD) where indicated. * $p < 0.05$ vs X/XO and
299 X/XO+CAT, one-way ANOVA, Tukey post hoc. (b) Time course (0-60 min) of X/XO $O_2^{\cdot-}$ generation was measured
300 using HPLC separation of 2-OHE⁺ and then plotted against the expected $O_2^{\cdot-}$ production. (c) Rose Bengal $O_2^{\cdot-}$
301 production rate per light dose. (d) Fluorescent protein (mCherry, tdKillerRed and SuperNova) $O_2^{\cdot-}$ production per
302 light dose. Data from (c) and (d) are derived from data presented in Fig. 2. * $p < 0.05$ SuperNova vs mCherry, ** p
303 < 0.05 SuperNova and tdKillerRed vs mCherry, two-way ANOVA, Bonferroni post hoc. Values are mean \pm SD for
304 $n = 3$ independent experiments.

305

306 ***Singlet oxygen quantum yield of fluorescent proteins***

307 Singlet oxygen sensor green (SOSG) specifically detects 1O_2 [4, 7, 27, 28] and does
308 not react with other ROS, such as $O_2^{\cdot-}$ or the hydroxyl radical, making it a suitable 1O_2 detector
309 under conditions where multiple ROS are being generated [29]. We assessed the 1O_2
310 production of the photosensitizers by measuring the relative change of SOSG fluorescence
311 and correcting for the bleaching rate of the individual fluorophores (Supplemental Fig. 2) [18].
312 Rose Bengal had the greatest SOSG fluorescence change with irradiation time (Fig. 4A)
313 relative to those of the fluorescent proteins (Fig. 4B). The Φ^1O_2 of the fluorescent proteins
314 were then calculated relative to the Rose Bengal reference Φ^1O_2 of 0.75 [18]. We determined
315 that SuperNova had the highest Φ^1O_2 at ~ 0.022 , while mCherry had the lowest Φ^1O_2 of
316 ~ 0.0057 (Table 1). This demonstrates that mCherry, KillerRed and SuperNova are each
317 capable of generating 1O_2 in an irradiation dose dependent manner.

318



319

320 Fig. 4. Singlet oxygen generation by photosensitizers in response to 561 nm irradiation. (a) Rose Bengal,
321 (b) tdKillerRed, SuperNova, mCherry and control (no photosensitizer) were irradiated with equal molar absorptivity
322 at 561 nm in the presence of 0.1 μM SOSG. The initial fluorescence reading (Ex 525 nm; Em 550 nm) was
323 subtracted from the post-illumination reading and presented as the relative fluorescence change. Values are mean
324 \pm SD for $n = 3$ independent experiments.

325

326 DISCUSSION

327 The main findings from this study are that the red fluorescent proteins tdKillerRed,
328 SuperNova, and mCherry each generate $\text{O}_2^{\cdot-}$ and $^1\text{O}_2$ via type I and II mechanisms,
329 respectively. We also report for the first time quantitative ROS quantum yields for tdKillerRed,
330 SuperNova and mCherry fluorescent proteins.

331 Genetically-encoded photosensitizers are used in a variety of biological applications to
332 generate ROS in a light-dependent manner. They have the advantage of being targeted to
333 precise regions in the cell to provide spatial control over ROS production [2]. However, their
334 precise ROS producing characteristics are often overlooked provided that a biological
335 phenotype has been observed. In contrast to $\Phi^1\text{O}_2$, very little is known about fluorescent
336 protein ΦO_2^- . This may be a result of the limited methods to selectively detect O_2^- , although
337 one study has reported the ΦO_2^- and $\Phi^1\text{O}_2$ of red fluorescent protein, TagRFP [4]. Using a
338 similar SOSG detection approach, the $\Phi^1\text{O}_2$ was estimated at 0.004, while the ΦO_2^- was
339 estimated at <0.0002 using DHE bleaching as a measure of O_2^- [4].

340 The first developed photosensitizer protein, KillerRed, was initially reported to make
341 O_2^- and $^1\text{O}_2$ [1, 10]. Subsequently, literature has suggested that the KillerRed
342 photosensitization mechanism selectively produces O_2^- and relies on the water channel to the
343 chromophore for its phototoxicity [10, 30]. Depending on the application, one type of ROS may
344 predominate in contributing to the light-induced effect. For example, $^1\text{O}_2$ played a role in
345 KillerRed CALI experiments [1], while O_2^- mediated phototoxicity [31]. While our results
346 demonstrate that both $^1\text{O}_2$ and O_2^- are capable of being produced, researchers should
347 consider which species is relevant to their particular biological application.

348 SuperNova was derived from KillerRed, and it would be reasonable to assume that the
349 photosensitization mechanisms would be similar. Accordingly, SuperNova has been thought
350 to produce O_2^- and $^1\text{O}_2$, as measured by 2-OHE⁺ formation [17] and ADPA photobleaching
351 [8], respectively. In the present study, SuperNova's comparatively larger ROS quantum yield
352 than KillerRed is consistent with previous reports of greater phototoxicity [8]. Specifically, at
353 916.5 J/cm^2 of fluence, we show that the SuperNova O_2^- production rate is ~1.6 fold higher
354 than KillerRed. However, the O_2^- production rate was not consistent across fluences tested,
355 and plateaued at the highest light dose tested. While the quantum yields provide a direct
356 comparison of the phototoxic mechanisms of the red fluorescent proteins tested, caution is
357 warranted when extrapolating these findings *in vivo*. The O_2 and pH gradients or endogenous

358 chromophores present in the cellular milieu can affect the ROS generation by
359 photosensitizers. For example, a high O₂ tension could favor ¹O₂ production, while hypoxic
360 conditions could favor O₂^{•-} production [32].

361 Unlike KillerRed and SuperNova that were derived from the jellyfish protein anm2CP,
362 mCherry was derived from the sea anemone protein DsRed. Owing to the structural
363 differences that exist due to their independent lineage, mCherry lacks a water channel,
364 suggesting that it would not be as phototoxic as KillerRed. Indeed, it is widely used in biological
365 applications under the assumption that it is photochemically inert. However, some previous
366 reports have also shown that mCherry can be phototoxic [33] and that it produces O₂^{•-} [8, 34]
367 and ¹O₂ [8] upon irradiation. Our present findings are in agreement with this and indicate that
368 mCherry actually displays similar $\Phi_{O_2^{\bullet-}}$ and Φ^1O_2 as 'professional' photosensitizer proteins.

369 The genetically-encoded photosensitizers display $\Phi_{O_2^{\bullet-}}$ and Φ^1O_2 that are orders of
370 magnitude lower than the chemical photosensitizer Rose Bengal. Yet, despite their lower
371 quantum yields, their ability to generate a biologically relevant effect is well established [1, 2,
372 8, 17]. Once formed by the excited chromophore, the superoxide anion must escape the
373 protein barrel structure in order to be released to the surrounding environment and react with
374 the ROS probe [10]. The protein barrel likely shields the release of ROS, potentially explaining
375 the lower observed $\Phi_{O_2^{\bullet-}}$ of the protein photosensitizers compared to Rose Bengal which can
376 directly release oxidants to the surrounding aqueous environment. Nevertheless, our current
377 Φ^1O_2 findings are generally in agreement with other fluorescent proteins that have been
378 reported to range from Φ^1O_2 0.004 to 0.030 [3]. Recently, optimized variants have reportedly
379 reached Φ^1O_2 ~0.6 [35]. New approaches are aimed at combining the large quantum yields of
380 chemical photosensitizers with the advantages of genetically-encoded photosensitizers [36].

381

382 **Conclusion**

383 Overall, we demonstrate that the red fluorescent proteins tdKillerRed, SuperNova and
384 mCherry are able to photosensitize $O_2^{\cdot-}$ and 1O_2 . Our studies provide $\Phi O_2^{\cdot-}$, Φ^1O_2 and rates of
385 $O_2^{\cdot-}$ production across light doses. Our findings will help elucidate mechanisms mediated by
386 phototoxic proteins and aid in the development of efficient or selective ROS production by
387 genetically-encoded photosensitizers [35, 37].

388

389 **ACKNOWLEDGEMENTS**

390 We thank the members of the mitochondrial research group at the University of
391 Rochester Medical Center for their valuable suggestions and contributions. AJT current
392 address: Institute for Physical Activity and Nutrition (IPAN), School of Exercise and Nutrition
393 Sciences, Deakin University, Burwood, VIC, Australia.

394

395 **Disclosure of funding:** This work was funded by a grant from the National Institutes of Health
396 to APW (R01 NS092558).

397

398 **Conflicts of interest:** There are no conflicts of interest to declare.

399 REFERENCES

- 400 [1] M.E. Bulina, D.M. Chudakov, O.V. Britanova, Y.G. Yanushevich, D.B. Staroverov, T.V. Chepurnykh,
401 E.M. Merzlyak, M.A. Shkrob, S. Lukyanov, K.A. Lukyanov, A genetically encoded photosensitizer,
402 *Nature biotechnology* 24(1) (2006) 95-9.
- 403 [2] A.P. Wojtovich, T.H. Foster, Optogenetic control of ROS production, *Redox biology* 2 (2014) 368-
404 76.
- 405 [3] A.J. Trewin, B.J. Berry, A.Y. Wei, L.L. Bahr, T.H. Foster, A.P. Wojtovich, Light-induced oxidant
406 production by fluorescent proteins, *Free radical biology & medicine* 128 (2018) 157-164.
- 407 [4] X. Ragas, L.P. Cooper, J.H. White, S. Nonell, C. Flors, Quantification of photosensitized singlet
408 oxygen production by a fluorescent protein, *Chemphyschem : a European journal of chemical physics*
409 and physical chemistry 12(1) (2011) 161-5.
- 410 [5] A.A. Krasnovsky, Jr., Primary mechanisms of photoactivation of molecular oxygen. History of
411 development and the modern status of research, *Biochemistry. Biokhimiia* 72(10) (2007) 1065-80.
- 412 [6] E.A. Souslova, K.E. Mironova, S.M. Deyev, Applications of genetically encoded photosensitizer
413 miniSOG: from correlative light electron microscopy to immunophotosensitizing, *Journal of*
414 *biophotonics* 10(3) (2017) 338-352.
- 415 [7] M.E. Barnett, T.M. Baran, T.H. Foster, A.P. Wojtovich, Quantification of light-induced miniSOG
416 superoxide production using the selective marker, 2-hydroxyethidium, *Free radical biology & medicine*
417 116 (2018) 134-140.
- 418 [8] K. Takemoto, T. Matsuda, N. Sakai, D. Fu, M. Noda, S. Uchiyama, I. Kotera, Y. Arai, M. Horiuchi, K.
419 Fukui, T. Ayabe, F. Inagaki, H. Suzuki, T. Nagai, SuperNova, a monomeric photosensitizing fluorescent
420 protein for chromophore-assisted light inactivation, *Scientific reports* 3 (2013) 2629.
- 421 [9] X. Shu, N.C. Shaner, C.A. Yarbrough, R.Y. Tsien, S.J. Remington, Novel chromophores and buried
422 charges control color in mFruits, *Biochemistry* 45(32) (2006) 9639-47.
- 423 [10] P. Carpentier, S. Violot, L. Blanchoin, D. Bourgeois, Structural basis for the phototoxicity of the
424 fluorescent protein KillerRed, *FEBS letters* 583(17) (2009) 2839-42.
- 425 [11] M. Westberg, L. Holmegaard, F.M. Pimenta, M. Etzerodt, P.R. Ogilby, Rational design of an
426 efficient, genetically encodable, protein-encased singlet oxygen photosensitizer, *Journal of the*
427 *American Chemical Society* 137(4) (2015) 1632-42.
- 428 [12] M.E. Bulina, K.A. Lukyanov, O.V. Britanova, D. Onichtchouk, S. Lukyanov, D.M. Chudakov,
429 Chromophore-assisted light inactivation (CALI) using the phototoxic fluorescent protein KillerRed,
430 *Nature protocols* 1(2) (2006) 947-53.
- 431 [13] T. Shibuya, Y. Tsujimoto, Deleterious effects of mitochondrial ROS generated by KillerRed
432 photodynamic action in human cell lines and *C. elegans*, *Journal of photochemistry and photobiology.*
433 *B, Biology* 117 (2012) 1-12.
- 434 [14] B. Wang, P.P. Van Veldhoven, C. Brees, N. Rubio, M. Nordgren, O. Apanasets, M. Kunze, M. Baes,
435 P. Agostinis, M. Fransen, Mitochondria are targets for peroxisome-derived oxidative stress in cultured
436 mammalian cells, *Free radical biology & medicine* 65 (2013) 882-894.
- 437 [15] L.W. Shao, R. Niu, Y. Liu, Neuropeptide signals cell non-autonomous mitochondrial unfolded
438 protein response, *Cell research* 26(11) (2016) 1182-1196.
- 439 [16] Z.X. Liao, Y.C. Li, H.M. Lu, H.W. Sung, A genetically-encoded KillerRed protein as an intrinsically
440 generated photosensitizer for photodynamic therapy, *Biomaterials* 35(1) (2014) 500-8.
- 441 [17] A.J. Trewin, L.L. Bahr, A. Almast, B.J. Berry, A.Y. Wei, T.H. Foster, A.P. Wojtovich, Mitochondrial
442 Reactive Oxygen Species Generated at the Complex-II Matrix or Intermembrane Space Microdomain
443 Have Distinct Effects on Redox Signaling and Stress Sensitivity in *Caenorhabditis elegans*, *Antioxid*
444 *Redox Signal* (2019).
- 445 [18] P.C. Lee, M.A. Rodgers, Laser flash photokinetic studies of rose bengal sensitized photodynamic
446 interactions of nucleotides and DNA, *Photochemistry and photobiology* 45(1) (1987) 79-86.
- 447 [19] E.E. Kelley, N.K. Khoo, N.J. Hundley, U.Z. Malik, B.A. Freeman, M.M. Tarpey, Hydrogen peroxide is
448 the major oxidant product of xanthine oxidase, *Free radical biology & medicine* 48(4) (2010) 493-8.

- 449 [20] E. Margoliash, N. Frohwirt, Spectrum of horse-heart cytochrome c, *Biochem J* 71(3) (1959) 570-2.
450 [21] J. Zielonka, J. Vasquez-Vivar, B. Kalyanaraman, Detection of 2-hydroxyethidium in cellular
451 systems: a unique marker product of superoxide and hydroethidine, *Nature protocols* 3(1) (2008) 8-
452 21.
453 [22] H. Zhao, J. Joseph, H.M. Fales, E.A. Sokoloski, R.L. Levine, J. Vasquez-Vivar, B. Kalyanaraman,
454 Detection and characterization of the product of hydroethidine and intracellular superoxide by HPLC
455 and limitations of fluorescence, *Proceedings of the National Academy of Sciences of the United States*
456 *of America* 102(16) (2005) 5727-32.
457 [23] S. Mitra, T.H. Foster, Photophysical parameters, photosensitizer retention and tissue optical
458 properties completely account for the higher photodynamic efficacy of meso-tetra-hydroxyphenyl-
459 chlorin vs Photofrin, *Photochemistry and photobiology* 81(4) (2005) 849-59.
460 [24] B. Kalyanaraman, M. Hardy, R. Podsiadly, G. Cheng, J. Zielonka, Recent developments in detection
461 of superoxide radical anion and hydrogen peroxide: Opportunities, challenges, and implications in
462 redox signaling, *Archives of biochemistry and biophysics* 617 (2017) 38-47.
463 [25] J. Zielonka, M. Hardy, B. Kalyanaraman, HPLC study of oxidation products of hydroethidine in
464 chemical and biological systems: ramifications in superoxide measurements, *Free radical biology &*
465 *medicine* 46(3) (2009) 329-38.
466 [26] R. Michalski, B. Michalowski, A. Sikora, J. Zielonka, B. Kalyanaraman, On the use of fluorescence
467 lifetime imaging and dihydroethidium to detect superoxide in intact animals and ex vivo tissues: a
468 reassessment, *Free radical biology & medicine* 67 (2014) 278-84.
469 [27] R. Ruiz-Gonzalez, A.L. Cortajarena, S.H. Mejias, M. Agut, S. Nonell, C. Flors, Singlet oxygen
470 generation by the genetically encoded tag miniSOG, *Journal of the American Chemical Society* 135(26)
471 (2013) 9564-7.
472 [28] A. Gollmer, J. Arnbjerg, F.H. Blaikie, B.W. Pedersen, T. Breitenbach, K. Daasbjerg, M. Glasius, P.R.
473 Ogilby, Singlet Oxygen Sensor Green(R): photochemical behavior in solution and in a mammalian cell,
474 *Photochemistry and photobiology* 87(3) (2011) 671-9.
475 [29] S. Kim, M. Fujitsuka, T. Majima, Photochemistry of singlet oxygen sensor green, *The journal of*
476 *physical chemistry. B* 117(45) (2013) 13985-92.
477 [30] S. Pletnev, N.G. Gurskaya, N.V. Pletneva, K.A. Lukyanov, D.M. Chudakov, V.I. Martynov, V.O.
478 Popov, M.V. Kovalchuk, A. Wlodawer, Z. Dauter, V. Pletnev, Structural basis for phototoxicity of the
479 genetically encoded photosensitizer KillerRed, *J Biol Chem* 284(46) (2009) 32028-39.
480 [31] E.O. Serebrovskaya, E.F. Edelweiss, O.A. Stremovskiy, K.A. Lukyanov, D.M. Chudakov, S.M. Deyev,
481 Targeting cancer cells by using an antireceptor antibody-photosensitizer fusion protein, *Proceedings*
482 *of the National Academy of Sciences of the United States of America* 106(23) (2009) 9221-5.
483 [32] R.C. Gilson, K.C.L. Black, D.D. Lane, S. Achilefu, Hybrid TiO₂ -Ruthenium Nano-photosensitizer
484 Synergistically Produces Reactive Oxygen Species in both Hypoxic and Normoxic Conditions, *Angew*
485 *Chem Int Ed Engl* 56(36) (2017) 10717-10720.
486 [33] R.L. Strack, D.E. Strongin, D. Bhattacharyya, W. Tao, A. Berman, H.E. Broxmeyer, R.J. Keenan, B.S.
487 Glick, A noncytotoxic DsRed variant for whole-cell labeling, *Nature methods* 5(11) (2008) 955-7.
488 [34] S. Hoffmann, M. Orlando, E. Andrzejak, C. Bruns, T. Trimbuch, C. Rosenmund, C.C. Garner, F.
489 Ackermann, Light-Activated ROS Production Induces Synaptic Autophagy, *The Journal of neuroscience*
490 *: the official journal of the Society for Neuroscience* 39(12) (2019) 2163-2183.
491 [35] M. Westberg, M. Bregnhøj, M. Etzerodt, P.R. Ogilby, No Photon Wasted: An Efficient and Selective
492 Singlet Oxygen Photosensitizing Protein, *The journal of physical chemistry. B* 121(40) (2017) 9366-
493 9371.
494 [36] J. He, Y. Wang, M.A. Missinato, E. Onuoha, L.A. Perkins, S.C. Watkins, C.M. St Croix, M. Tsang, M.P.
495 Bruchez, A genetically targetable near-infrared photosensitizer, *Nature methods* 13(3) (2016) 263-8.
496 [37] M. Westberg, M. Etzerodt, P.R. Ogilby, Rational design of genetically encoded singlet oxygen
497 photosensitizing proteins, *Curr Opin Struct Biol* 57 (2019) 56-62.

498

500 **TABLE 1:**

501 Superoxide and singlet oxygen quantum yield of mCherry, tdKillerRed, and SuperNova.

Fluorescent proteins	O ₂ ⁻ Quantum yield ($\phi_{O_2^-}$)	¹ O ₂ Quantum yield (ϕ^1O_2)
mCherry	0.00120±0.000044	0.0057±0.00027
tdKillerRed	0.00097±0.000042	0.0076±0.00026
SuperNova	0.00150±0.000016	0.0220±0.00180

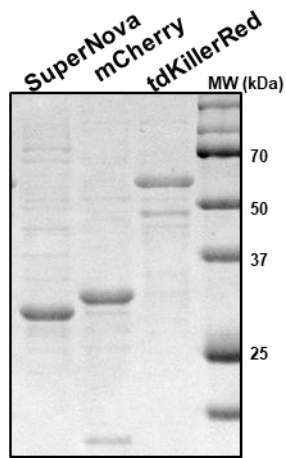
502

503 Data are mean ± SD for n=3 independent experiments

504

505 Supplemental Fig. 1.

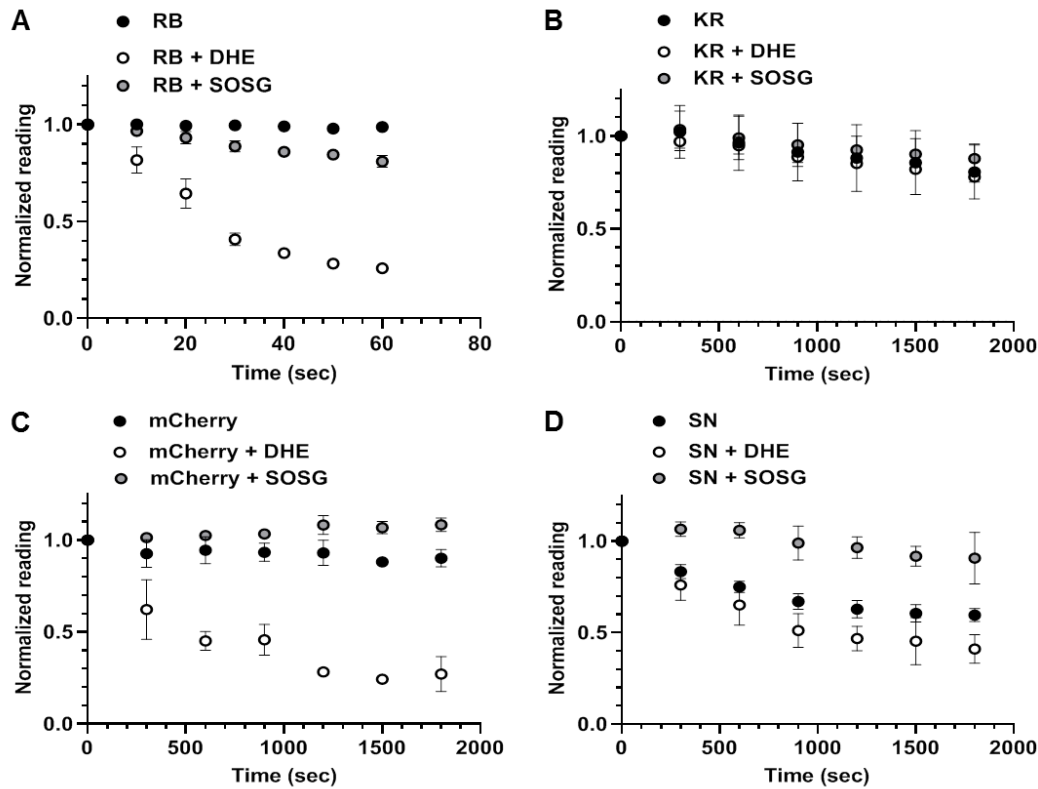
Fig S1



Coomassie stain

506

507 Supplemental Fig. 1. **Purified fluorescent proteins.** Purified SuperNova, mCherry, and tandem KillerRed protein
508 were denatured in buffer containing 100 mM Tris HCl, 4% w/v SDS, 10% v/v glycerol, 0.2% w/v bromophenol blue,
509 2% v/v β -mercaptoethanol then heated for 5 min at 95°C before separation by SDS-PAGE (10 μ g per lane) and
510 then stained with coomassie blue.



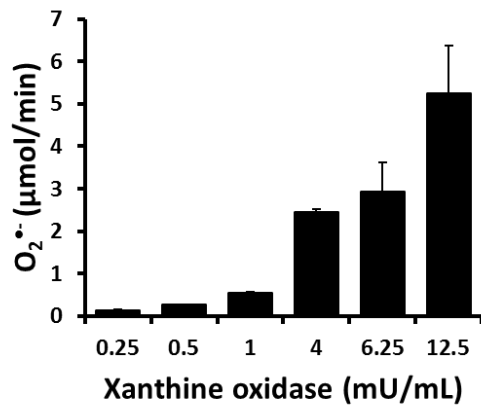
511

512 Supplementary Fig. 2. **Photobleaching rates of photosensitizers with DHE or SOSG.** (A) Rose Bengal, (B)
513 KillerRed, (C) mCherry, and (D) SuperNova alone or in the presence of dihydroethidium (DHE) or Singlet Oxygen
514 Sensor Green (SOSG). The cumulative fluorescence (photosensitizer alone or with DHE) or cumulative
515 absorbance (photosensitizer with SOSG) was measured (0-60 sec for Rose Bengal; 0-30 min for KillerRed,
516 mCherry, and SuperNova) following irradiation at 561 nm. Data were then normalized to baseline after bleaching
517 fit correction using MATLAB. Data are N = 3, mean \pm SD.

518

519

520



521

522

523 Supplementary Fig. 3. **Dose dependent superoxide production of xanthine oxidase.** Xanthine oxidase (0.25,
524 0.5, 1, 4, 6.25 and 12.5 mU/mL) superoxide production was assessed with in the presence xanthine (1mM) using
525 cytochrome c reduction. Data are N = 4 independent values, mean ±SD.

526